Thermal Decomposition of 4-Methylpyrimidine. Experimental Results and Kinetic Modeling

Assa Lifshitz,* Aya Suslensky, and Carmen Tamburu

Department of Physical Chemistry, The Hebrew University, Jerusalem 91904, Israel

Received: October 31, 2000; In Final Form: January 26, 2001

The decomposition of 4-methylpyrimidine was studied behind reflected shock waves in a pressurized driver single-pulse shock tube over the temperature range 1160−1330 K at overall densities of $\sim 3 \times 10^{-5}$ mol/cm^3. A plethora of decomposition products, both with and without nitrogen was found in the post-shock mixtures. They were HCN, CH_3CN, C_2H_3CN, pyrimidine, C_2H_5CN, *cis*- and *trans*-$CH_3CH{=}CHCN$, $CH_2{=}CHCH_2CN$, $CH{\equiv}C{-}CN$, and C_2N_2, among the nitrogen containing products, and CH_4, C_2H_2, $CH_3C{\equiv}CH$, C_2H_6, $CH_2{=}C{=}CH_2$, and C_2H_4 as products without nitrogen. It is suggested that the decomposition of 4-methylpyrimidine has two major initiation steps. (1) An ejection of a hydrogen atom from the methyl group that is connected to the ring, $C_4H_3N_2{-}CH_3 \rightarrow C_4H_3N_2{-}CH_2^{\bullet} + H^{\bullet}$, and (2) split of the methyl group from the ring, $C_4H_3N_2{-}CH_3 \rightarrow C_4H_3N_2^{\bullet} + CH_3^{\bullet}$. The ejection of H atom from the ring is much slower and does not contribute much to the total rate. The H atoms and methyl radicals initiate a chain mechanism by abstraction of an H atom from the methyl group and by dissociative attachment of an H atom and removal of a methyl group from the ring. The pyrimidyl ($C_4H_3N_2^{\bullet}$) and methylene pyrimidine ($C_4H_3N_2{-}CH_2^{\bullet}$) radicals decompose by ring cleavage followed by breakdown of the open-ring radical. The total decomposition of 4-methylpyrimidine in terms of a first-order rate constant is given by $k_{\text{total}} = 10^{15.37} \exp(-83.5 \times 10^3/RT)$ s^{-1}. A reaction scheme containing 33 species and 91 elementary reactions was constructed to account for the observed product distribution. A discussion on the decomposition mechanism is presented.

I. Introduction

The thermal reactions of pyrimidine and pyrazine have been studied in the past using shock tubes as the heating device, with a variety of diagnostic techniques.[1−4] It has been suggested that in both isomers the decomposition begins with an ejection of a hydrogen atom from the ring followed by opening of the ring in β positions to the radical site and fragmentation by successive β-scissions with and without hydrogen atom shifts. Overall reaction schemes for the decomposition have been composed and computer modeling was run to support the suggested mechanisms. The addition of a methyl group to pyrimidine, to form methyl pyrimidine, introduces two additional bonds: $-CH_2{-}H$ and $C{-}CH_3$. These bonds are considerably weaker than the C−H bonds in pyrimidine even though some of the radicals that are formed are resonance stabilized by adjacent nitrogen atoms. Owing to the formation of different radicals in the process of initiation, the decomposition pathways are different. Also being a larger molecule with a methyl group, production of more products is expected.

In the present investigation the thermal reactions of 4-methylpyrimidine are studied and a detailed mechanism for the production of the many products that are formed is suggested. A kinetic scheme is composed and computer modeling is run to support the suggested mechanism.

II. Experimental Section

1. Apparatus. The decomposition of 4-methylpyrimidine was studied behind reflected shocks in a pressurized driver, heated, 52 mm i.d.. single pulse shock tube. The tube, made of electropolished stainless steel tubing, was heated and maintained at 120 °C with an accuracy of ±1 °C. The driven section, was 4 m long and was divided in the middle by a 52 mm i.d. ball valve. The driver had a variable length up to a maximum of 2.7 m and could be varied in small steps in order to obtain the best cooling conditions. A 36 L dump tank was connected to the driven section at 45° angle near the diaphragm holder in order to prevent reflection of transmitted shocks. The driven section was separated from the driver by "Mylar" polyester film of various thickness depending upon the desired shock strength.

After pumping down the tube to approximately 3×10^{-5} Torr, the reaction mixture was introduced into the section between the valve and the end plate and pure argon into the section between the diaphragm and the valve, including the dump tank. After running an experiment, samples were injected from the downstream end of the driven section into a Hewlett-Packard model 5890 gas chromatograph operating with 2 Porapak-N columns using flame ionization (FID) and nitrogen-phosphor (NPD) detectors. All the transfer tubes and the injection system were maintained at 120 °C.

Reflected shock temperatures were calculated from the extent of decomposition of 1,1,1-trifluoroethane which was added to the reaction mixture and served as an internal standard. Its decomposition to $CH_2{=}CF_2 + HF$ is a first-order unimolecular reaction with a rate constant[5]: $k_{\text{first}} = 10^{14.85}\exp(-74.05 \times 10^3/RT)$ s^{-1}.

Reflected shock temperatures were calculated from the relation

$$T = -(E/R)\Big/\left[\ln\left\{-\frac{1}{At}\ln(1-\chi)\right\}\right] \qquad \text{(I)}$$

where E is the activation energy of the HF elimination, A is its

10.1021/jp0040392 CCC: \$20.00

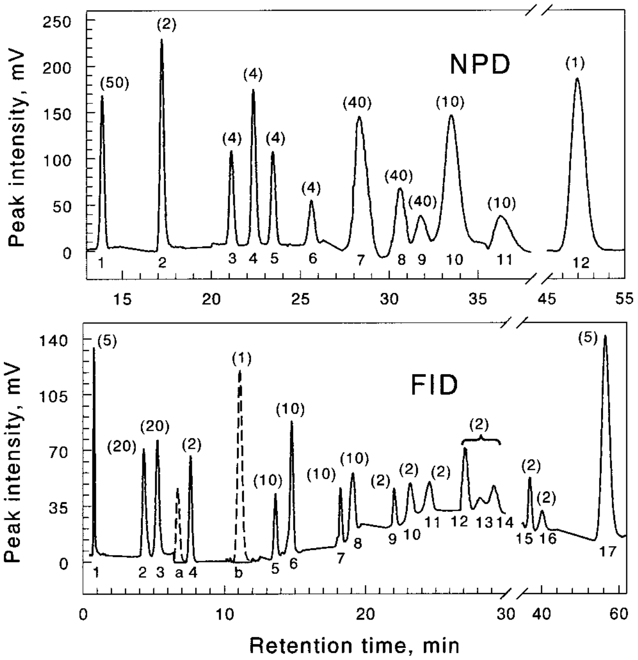

Figure 1. Gas chromatograms of a post-shock mixture of 0.25% 4-methylpyrimidine in argon heated to 1296 K, taken on NPD (top) and FID (bottom). The numbers on top of the peaks indicate multiplication factors. The products are (**NPD**) 1. C_2N_2 2. HCN 3. $CH{\equiv}C{-}CN$ 4. CH_3CN 5. C_2H_3CN 6. C_2H_5CN 7. *cis*-$CH_3CH{=}CHCN$ 8. $CH_2{=}CHCH_2CN$ 9. *trans*-$CH_3CH{=}CHCN$ 10. pyrimidine 11. pyrazine 12. 4-methylpyrimidine. (**FID**) 1. CH_4. 2. C_2H_4. 3. C_2H_6 4. C_2H_2. 5. $CH_2{=}C{=}CH_2$. 6. $CH_3C{\equiv}CH$. 7. C_2N_2. 8. HCN. 9. $CH{\equiv}C{-}CN$. 10. CH_3CN. 11. $CH_2{=}CHCN$. 12. *cis*-$CH_3CH{=}CHCN$. 13. $CH_2{=}CHCH_2$-CN. 14. *trans*-$CH_3CH{=}CHCN$. 15. Pyrimidine. 16. Pyrazine. 17. 4-Methylpyrimidine (a) $CH_2{=}CF_2$, (b) CH_3CF_3.

preexponential factor, t is the reaction dwell time, and χ is the extent of decomposition defined as

$$\chi = [CH_2{=}CF_2]_t/([CH_2{=}CF_2]_t + [CH_3CF_3]_t) \qquad (II)$$

The additional reflected shock parameters were calculated from the measured incident shock velocities using the three conservation reactions and the ideal gas equation of state. Dwell times of approximately 2 ms were measured with an accuracy of ~5%. Cooling rates were approximately 5×10^{-5} K/s.

2. Materials and Analysis. Reaction mixtures containing 0.25% 4-methylpyrimidine and 0.25% 1,1,1-trifluoroethane diluted in argon were prepared manometrically and stored in 12 L glass bulbs at 700 Torr. Both the bulbs and the line were pumped down to $\sim 10^{-5}$ Torr before the preparation of the mixtures. 4-methylpyrimidine was obtained from Aldrich Chemical Co. and was listed as 97% pure. However, chromatograms of unshocked samples did not show any of the products that appeared in the shocked samples. The argon used was Matheson ultrahigh purity grade, listed as 99.9995%, and the helium was Matheson pure grade listed as 99.999%.

The gas chromatographic analyses of the post-shock mixtures were performed on two Porapak-N columns using flame ionization and nitrogen-phosphor detectors. The initial column temperature of 35 °C was gradually elevated to 190 °C in an analysis which lasted approximately 1 h. Typical chromatograms of 0.25% 4-methylpyrimidine in argon of a shock heated mixture to 1296 K are shown in Figure 1.

3. Determination of Product Concentration. The concentrations of the reaction products $C_5(\mathrm{pr})_i$ were calculated from their GC peak areas from the following relations:

$$C_5(\mathrm{pr})_i = A(\mathrm{pr}_i)_t/S(\mathrm{pr}_i)\ \{C_5(\text{4-mpyrim.})_0/A(\text{4-mpyrim.}) \qquad (III)$$

$$C_5(\text{4-mpyrim.})_0 = \{p_1 \times \%(\text{4-mpyrim.})\rho_5/\rho_1\}/100RT_1 \qquad (IV)$$

$$A(\text{4-mpyrim.})_0 = A(\text{4-mpyrim.})_t + {}^1/_5 \sum N(\mathrm{pr}_i) \times A(\mathrm{pr}_i)_t/S(\mathrm{pr}_i) \qquad (V)$$

In these relations, $C_5(\text{4-mpyrim.})_0$ is the concentration of 4-methylpyrimidine behind the reflected shock wave prior to decomposition and $A(\text{4-mpyrim.})_0$ is the calculated GC peak area of 4-methylpyrimidine prior to decomposition (eq V) where $A(\mathrm{pr}_i)_t$ is the peak area of a product i in the shocked sample, $S(\mathrm{pr}_i)$ is its sensitivity relative to 4-methylpyrimidine, and $N(\mathrm{pr}_i)$ is the number of its carbon atoms. ρ_5/ρ_1 is the compression behind the reflected shock wave and T_1 is room temperature, 120 °C in this study.

The identification of the reaction products was based on their GC retention times and was assisted also by a Hewlett-Packard model 5970 mass selective detector. The sensitivities of the various products to the FID and NPD were determined relative to 4-methylpyrimidine from standard mixtures. The areas under the GC peaks were integrated with a Spectra Physics model SP4200 computing integrator and were transferred after each analysis to a PC for data reduction and graphical presentation.

III. Results

To determine the distribution of reaction products, some 30 tests were run with mixtures containing 0.25% 4-methylpyrimidine in argon, covering the temperature range 1160−1330 K. Extents of pyrolysis starting from less than one hundredth of one percent were determined for many of the products. Details of the experimental conditions and the distribution of reaction products are given in Table 1. The percent of a given product in the Table, corresponds to its mole fraction in the post-shock mixture (not including Ar and H_2), irrespective of the number of its carbon atoms.

The balance of nitrogen vs carbon in the decomposition products is shown in Figure 2. One-half the sum of the concentrations of all the nitrogen containing products each multiplied by the number of its nitrogen atoms, are plotted against one-fifth the sum of the concentrations of all the products each multiplied by the number of its carbon atoms. The diagonal in the figure represents a perfect mass balance. As can be seen mass balance is maintained.

Figure 3 shows the rate constant for the overall decompositions of 4-methylpyrimidine, calculated as a first-order rate constant from the relation:

$$k_{\mathrm{total}} = -\ln\{[\text{4-methylpyrimidine}]_t/[\text{4-methylpyrimidine}]_0\}/t \qquad (VI)$$

The value obtained is $k_{\mathrm{total}} = 10^{15.37}\exp(-83.5 \times 10^3/RT)$ s^{-1}, where R is expressed in units of cal/(K mol). Figure 4 shows, as an example, Arrhenius plots of the first-order production rate of HCN, CH_4 and C_2N_2, calculated from the relation:

$$k_{\mathrm{product}} = \frac{[\mathrm{product}]_i}{[\text{4-methypyrim}]_0 - [\text{4-methypyrim}]_t} k_{\mathrm{tota}} \qquad (VII)$$

Note that the values calculated from Eq. VII correspond to the production rates and not to the depletion rate of the reactant

TABLE 1: Product Distribution in Percent

(a) Hydrocarbons

no.	T_5 K	$C_5 \times 10^5$ mol/cm^3	t (ms)	CH_4	C_2H_4	C_2H_6	C_2H_2	allene	propyne
1	1160	2.70	2	0.037			0.022		
2	1167	2.78	2.11	0.033		0.0076	0.015		
3	1172	2.78	1.90	-			0.023		
4	1173	2.97	1.95	-			0.022		0.0030
5	1174	2.86	1.90	0.038			0.014		
6	1197	2.77	1.91	0.020	0.0076	0.025	0.064	0.0033	0.0080
7	1200	2.76	2.08	0.169	0.043	0.020	0.067		
8	1202	2.76	2.08	0.116		0.0067	0.052		
9	1203	2.83	1.93	0.103	0.012	0.017	0.058	0.0029	0.0079
10	1205	2.54	1.85	0.061			0.062	0.00090	0.0074
11	1207	2.76	1.94	0.151		0.016	0.076		
12	1213	2.74	1.98		0.0084	0.021	0.091	0.0043	0.013
13	1238	2.56	2.04	0.135	0.016	0.019	0.126	0.015	0.027
14	1247	2.47	2.10	0.174	0.015	0.019	0.154	0.011	0.029
15	1249	2.57	2	0.233	0.012	0.011	0.198	0.015	0.034
16	1252	2.59	2	0.135	0.020	0.037	0.204	0.017	0.039
17	1252	2.58	2.08	0.296	0.075	0.053	0.352	0.030	0.064
18	1260	2.27	2.09	0.245	0.024	0.026	0.226	0.018	0.048
19	1266	2.42	2.02	0.474	0.0083	0.070	0.378	0.025	0.084
20	1266	2.44	2.11	0.176	0.024	0.032	0.232	0.018	0.044
21	1278	2.31	2.04	0.429	0.078	0.052	0.446	0.042	0.091
22	1281	2.59	2.12	0.495		0.077	0.505	0.050	0.112
23	1284	2.36	2	0.536	0.081	0.119	0.692	0.064	0.146
24	1296	2.36	1.90	0.554	0.076	0.078	0.668	0.063	0.148
25	1301	2.30	2.02	0.908	0.104	0.121	1.04	0.099	0.221
26	1304	2.32	2.07	0.824	0.108	0.094	1.06	0.098	0.220
27	1321	2.19	2.11	1.88	0.236	0.245	2.56	0.237	0.545
28	1337	2.22	1.98	3.02	0.671	0.462	5.05	0.413	0.888
29	1341	2.22	2.03	2.24	0.471	0.465	4.19	0.375	0.797

(b) Nitrogen-Containing Species

no.	T_5	$C_5 \times 10^5$ mol/cm^3	t (ms)	methylpyrimidine	C_2N_2	HCN	CH/CCN	CH_3CN	C_2H_3CN	C_2H_5CN	$CH_3{-}CH{=}CH{-}CN$	pyrimidine
1	1160	2.70	2	99.82	0.00091	0.059	0.011	0.024	0.0075	0.0052	0.012	0.0065
2	1167	2.78	2.12	99.53	0.0012	0.091	0.0067	0.043	0.014	0.022	0.092	0.141
3	1172	2.78	1.90	99.69	0.0017	0.174	0.015	0.038	0.023	0.033		
4	1173	2.97	1.95	99.75	0.0011	0.112	0.010	0.051	0.013	0.028	0.0069	
5	1174	2.86	1.90	99.79	0.00066	0.073	0.0070	0.041	0.014	0.018		
6	1197	2.77	1.91	99.33	0.0026	0.288	0.025	0.075	0.033	0.036	0.038	0.047
7	1200	2.76	2.08	98.83	0.0033	0.381	0.026	0.095	0.048	0.027	0.093	0.198
8	1202	2.76	2.08	99.28	0.0036	0.197	0.031	0.047	0.044	0.032	0.047	0.143
9	1203	2.83	1.93	98.61	0.0030	0.443	0.023	0.182	0.063	0.093	0.142	0.236
10	1205	2.54	1.85	99.33	0.0026	0.369	0.024	0.074	0.038	0.034		
11	1207	2.76	1.94	98.93	0.0049	0.442	0.036	0.102	0.067	0.064	0.055	0.058
12	1213	2.74	1.98	99.06	0.0041	0.50	0.032	0.138	0.056	0.073		
13	1238	2.56	2.04	98.16	0.0067	0.872	0.046	0.194	0.10	0.090	0.108	0.090
14	1247	2.47	2.10	97.86	0.0063	1.11	0.054	0.247	0.136	0.113	0.061	
15	1249	2.57	2	97.65	0.0076	1.20	0.054	0.197	0.101	0.082	0.129	0.071
16	1252	2.59	2	97.59	0.0091	1.36	0.065	0.158	0.109	0.060	0.129	0.064
17	1252	2.58	2.08	95.65	0.018	2.08	0.109	0.408	0.214	0.199	0.204	0.241
18	1260	2.27	2.09	96.84	0.0083	1.61	0.077	0.364	0.205	0.163	0.112	
19	1266	2.42	2.02	94.96	0.019	2.23	0.102	0.516	0.298	0.301	0.350	0.165
20	1266	2.44	2.11	96.19	0.013	1.70	0.086	0.397	0.220	0.198	0.328	0.349
21	1278	2.31	2.04	93.51	0.024	3.26	0.158	0.636	0.357	0.256	0.420	0.251
22	1281	2.59	2.12	94.40	0.025	2.86	0.169	0.376	0.293	0.220	0.358	0.054
23	1284	2.36	2	91.75	0.026	4.59	0.201	0.555	0.369	0.237	0.465	0.166
24	1296	2.36	1.90	90.76	0.035	4.76	0.241	0.831	0.530	0.342	0.676	0.242
25	1301	2.30	2.02	87.75	0.034	6.75	0.285	0.862	0.567	0.323	0.729	0.214
26	1304	2.32	2.07	89.15	0.040	5.39	0.269	0.883	0.580	0.344	0.682	0.259
27	1321	2.19	2.11	73.45	0.062	13.97	0.722	1.86	1.38	0.639	1.79	0.439
28	1337	2.22	1.98	54.53	0.101	23.64	1.27	3.18	2.47	0.996	2.78	0.533
29	1341	2.22	2.03	57.73	0.108	22.50	1.13	3.16	2.36	1.04	2.87	0.567

due to the production of a given product. Values of E obtained from the slopes of the lines and their corresponding preexponential factors are summarized in Table 2. Since the production of all the stable products is associated with free radical reactions, their Arrhenius parameters do not correspond to the parameters of true first-order rate constants. They do provide, however, a convenient way to summarize general rates.

IV. Discussion

1. Reaction Mechanism. ***A. Initiation.*** There are in principle five initiation steps in the decomposition of 4-methylpyrimidine that can produce active free radicals and unstable intermediates whose decomposition can lead to a free radical mechanism. Three steps involve ejection of hydrogen atoms from three

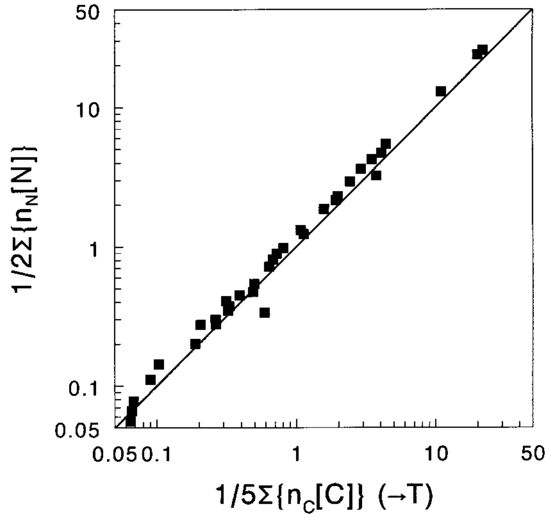

Figure 2. Nitrogen−Carbon mass balance among the decomposition products. The 45° line indicates a perfect mass balance. Nitrogen−carbon mass balance is maintained.

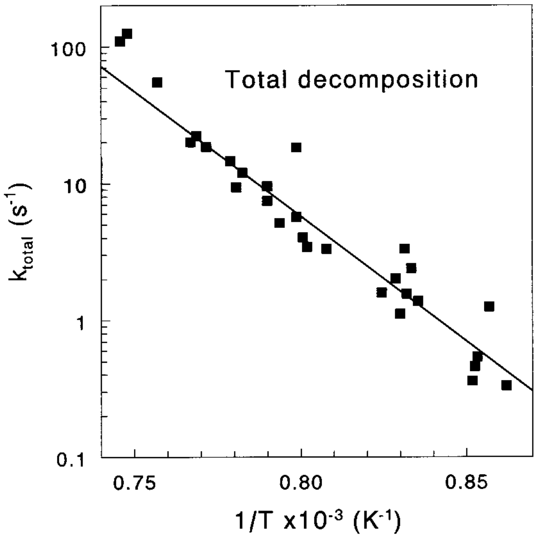

Figure 3. Arrhenius plot of a first-order rate constant for the overall decomposition of 4-methylpyrimidine. The rate constant is calculated from the relation: $k_{total} = -\ln\{[\text{4-methylpyrim.}]_t/[\text{4-methylpyrim.}]_0\}/t$. The value obtained is $k_{total} = 10^{15.37}\exp(-83.5 \times 10^3/RT)$ s^{-1}.

locations in the ring:

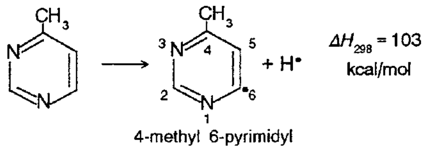

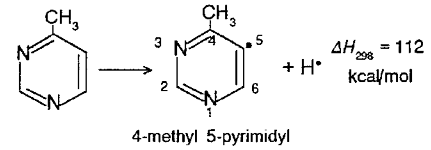

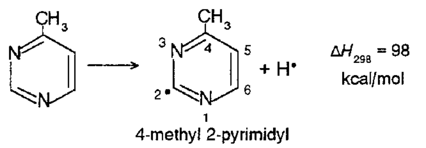

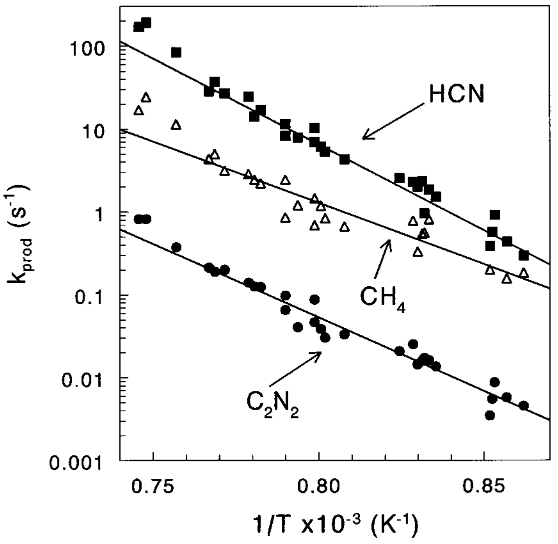

Figure 4. Arrhenius plots for the formation of HCN, CH_3CN and C_2H_4 calculated from the relation $k_{product} = ([\text{product}]_t/[\text{reactant}]_0 - [\text{reactant}]_t)k_{total}$.

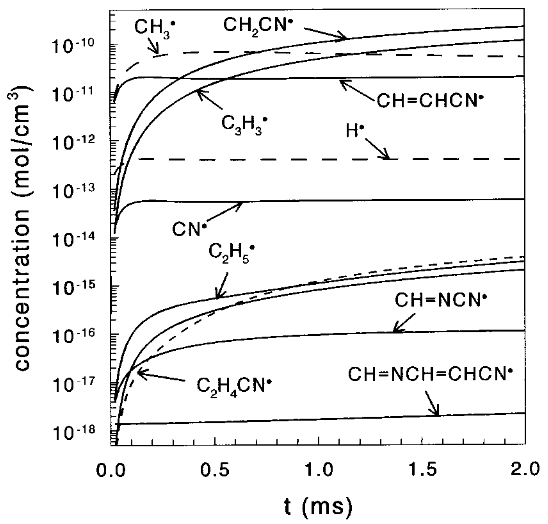

Figure 5. Profiles of reactive free radicals calculated for 1250 K. Six free radicals of the highest concentrations were introduced into the kinetic scheme.

TABLE 2: First-Order Arrhenius Parameters for Formation Rate

product	log(A, s^{-1})	E (kcal/mol)
methylpyrimidine (total dec.)	15.37	83.5
pyrimidine		
HCN	17.42	95.0
CH_3CN	13.05	73.7
C_2H_3CN	14.23	82.0
C_2H_5CN	11.33	65.8
CH≡CCN	13.43	79.2
C_2N_2	12.95	81.7
CH_3−CH=CHCN	16.83	96.2
CH_4	11.97	67.8
C_2H_4		
C_2H_6	10.40	63.7
C_2H_2	15.20	86.6
a-C_3H_4	17.18	104.4
p-C_3H_4	19.24	113.9

Owing to the resonance stabilization by adjacent nitrogen atoms, out of the three possible H atom ejections from the ring the 4-methyl-2-pyrimidyl radical is considerable more stable than both the 5- and 6- isomers. Its production is associated with a lower activation energy and is thus much faster. Out of the three H atom ejections from the ring we considered only the production and decomposition of 4-methyl-2-pyrimidyl.

The other two steps are ejection of a hydrogen atom from the methyl group, and removal of the methyl group from the ring. The activation energy for the H atom ejection from the methyl group is considerably lower than the activation energy for an ejection of a sp^2 hydrogen from the pyrimidine ring, even in comparison to the production of the 2-pyrimidyl radical. The removing of a methyl group has also a lower barrier than removing a hydrogen atom from the ring. We therefore considered three initiation steps in establishing the free radical mechanism: formation of 4-methylene pyrimidine, 4-methyl-2-pyrimidyl, and 4-pyrimidyl.

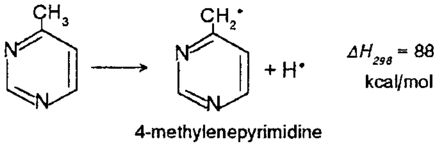

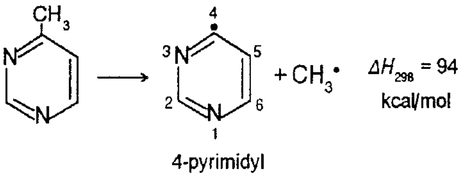

Following these initiation steps, hydrogen atom and methyl group attack on the reactant and eventually on the products, and unimolecular decompositions of the above-mentioned unstable intermediates are the significant steps in the mechanism of the decomposition.

B. Decomposition of Unstable Intermediates. a. 4-Methylene Pyrimidine. The attack of methyl radicals on the methyl group in 4-methylpyrimidine produces methane which is a major product among the species not containing nitrogen, leaving the radical 4-methylene pyrimidyl: The result of H atom attack on 4-methylpyrimidine is either an abstraction to produce mainly $C_4H_3N_2-CH_2^•$ and molecular hydrogen, or dissociative recombination to yield pyrimidine and a methyl radical.

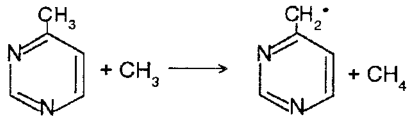

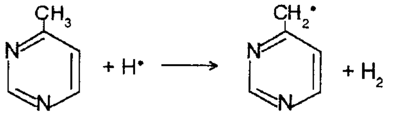

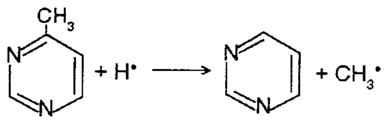

In comparison to the unstable radical intermediates, pyrimidine is a stable molecule—its only decomposition is ejection of a hydrogen atom, mainly from the position between the two nitrogen atoms in the ring. We have included in the present scheme a subscheme describing the decomposition of pyridine taken from the work of Kiefer et al. with some modifications which are relevant to the present investigation.

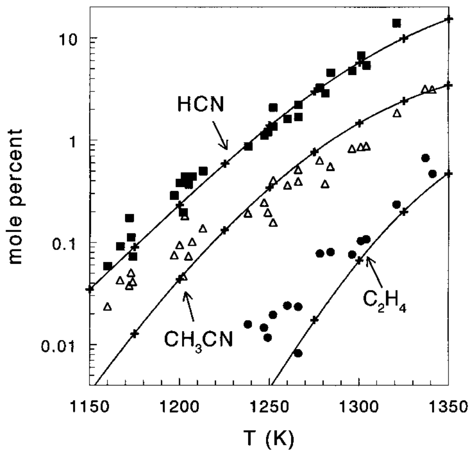

Figure 6. Calculated and experimental yields of HCN, CH_3CN and C_2H_4 plotted against the temperature. The lines are the best fit through the calculated points obtained at 25 K intervals, shown here as (+).

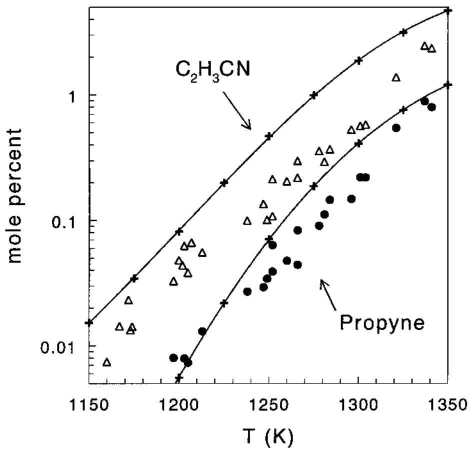

Figure 7. Calculated and experimental yields of C_2H_3CN and $CH_3C\equiv CH$ plotted against the temperature. The lines are the best fit through the calculated points obtained at 25 K intervals, shown here as (+).

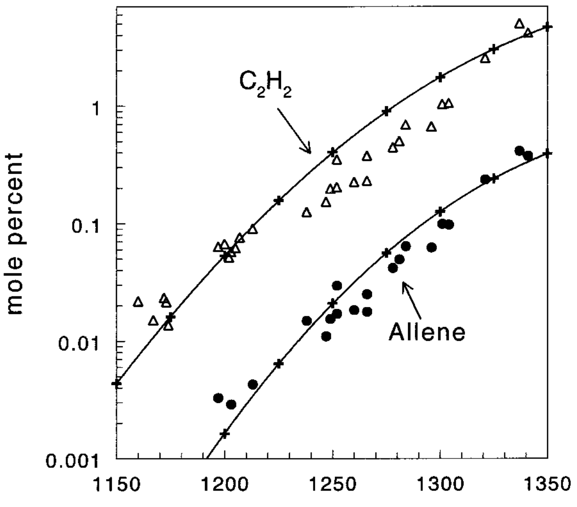

Figure 8. Calculated and experimental yields of C_2H_2 and $CH_2=C=CH_2$ plotted against the temperature. The lines are the best fit through the calculated points obtained at 25 K intervals, shown here as (+).

Most of the nitrogen containing species are obtained by the decomposition of 4-methylene pyrimidine ($C_4H_3N_2-CH_2^•$). The latter that is iso-electronic to benzyl radical exists in three resonance structures. It opens to a noncyclic compound,

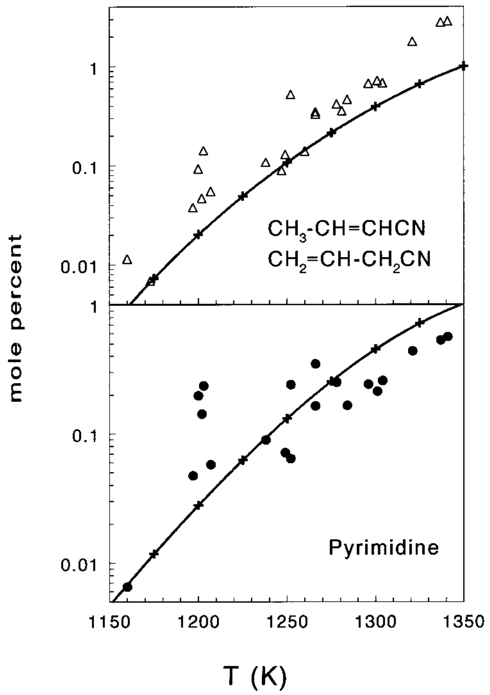

Figure 9. Calculated and experimental yields of the sum of $CH_3CH=CHCN$ and $CH_2=CHCH_2CN$, and pyrimidine plotted against the temperature. The lines are the best fit through the calculated points obtained at 25 K intervals, shown here as (+).

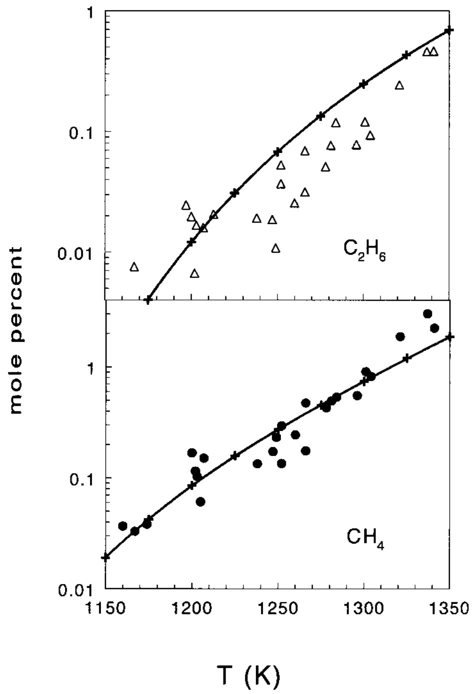

Figure 10. Calculated and experimental yields of C_2H_6 and CH_4 plotted against the temperature. The lines are the best fit through the calculated points obtained at 25 K intervals, shown here as (+).

l-$C_4H_3N_2{-}CH_2^{\bullet}$, that will decompose to smaller segments by

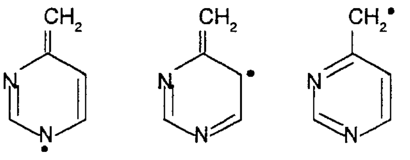

successive *β*-scissions. From all the possible decomposition pathways, the final products are

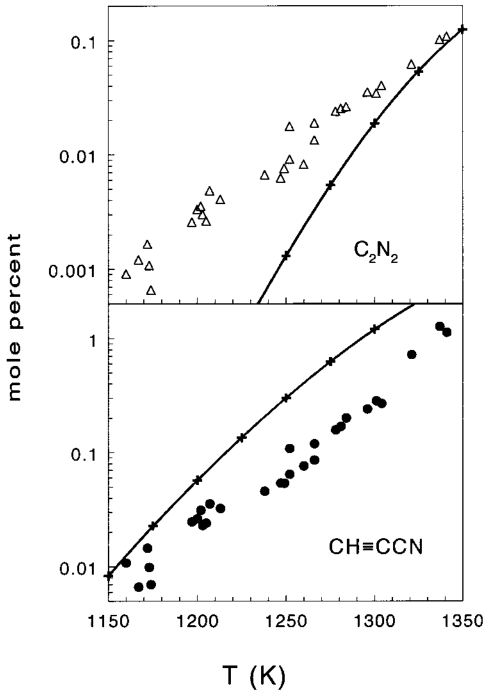

Figure 11. Calculated and experimental yields of C_2N_2 and $CH{\equiv}C{-}CN$ plotted against the temperature. The lines are the best fit through the calculated points obtained at 25 K intervals, shown here as (+).

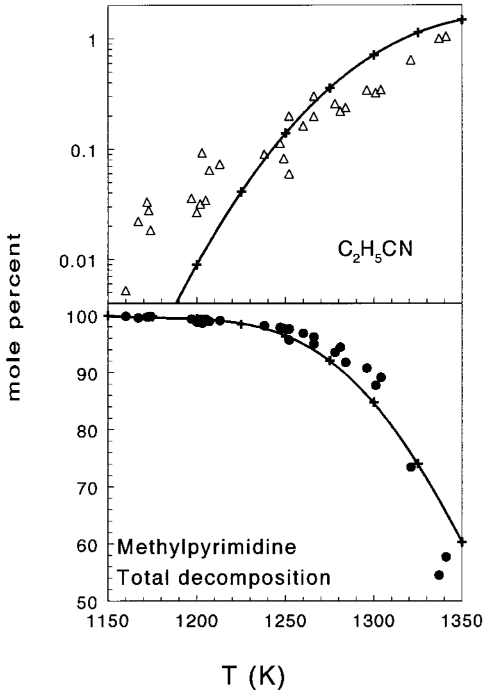

Figure 12. Calculated and experimental yields of C_2H_5CN and the total decomposition of 4-methylpyrimidine plotted against the temperature. The lines are the best fit through the calculated points obtained at 25 K intervals, shown here as (+).

$$l\text{-}C_4H_3N_2{-}CH_2^{\bullet} \rightarrow C_2H_3^{\bullet} + 2HCN \qquad (12)$$

$$l\text{-}C_4H_3N_2{-}CH_2^{\bullet} \rightarrow CH_2CN^{\bullet} + C_2H_3CN \qquad (13)$$

$$l\text{-}C_4H_3N_2{-}CH_2^{\bullet} \rightarrow CH_2CN^{\bullet} + HCN + C_2H_2 \qquad (14)$$

Because information is not available on the precise pathways in the decomposition of this species, we have treated each pathway as one single global process and inserted these three reactions to the reaction scheme as single step reactions.

b. 4-Methyl-2-pyrimidyl. This species is obtained by ejection or abstraction of a H atom from position 2 in the ring, namely, from the position between the two nitrogen atoms: Similar to

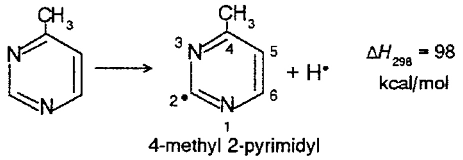

4-methylene pyrimidine it will open by breaking two C−N bonds in the β-position on the ring to form *l*- $C_4H_2N_2^\bullet$-CH_3 and will further fragmentize to smaller species by successive β-scissions. From all the possible decomposition pathways the final products are

$$l\text{-}C_4H_2N_2^\bullet{-}CH_3 \rightarrow CH_3{-}C{\equiv}CH + HCN + CN^\bullet \quad (16)$$

$$l\text{-}C_4H_2N_2^\bullet\text{-}CH_3 \rightarrow CH_3{-}C{\equiv}CH + CHNCN^\bullet \quad (17)$$

$$l\text{-}C_4H_2N_2^\bullet\text{-}CH_3 \rightarrow C_2H_2 + CH_3CN + CN^\bullet \quad (18)$$

As has been done previously with *l*-$C_4H_3N_2{-}CH_2^\bullet$, we treated these three global reactions as a single step reactions.

c. 2- and 4-Pyrimidyl. 2-Pyrimidyl is obtained by H atom ejection from pyrimidine. The latter is obtained by dissociative recombination of H atoms with 4-methylpyrimidine (reaction 19) to yield pyrimidine and a methyl radical. It decomposes by a series of β-scissions. We have adopted the mechanism suggested by Mackie et al.[2] and Kiefer et al.[1−3] in their study on the decomposition of diazines. The decomposition yields mainly C_2H_2 and $CHNCH^\bullet$.

4-Pyrimidyl is obtained by rupture of the C−CH_3 bond in 4-methylpyrimidine. Its production from the dissociation of pyrimidine is practically negligible. It has been suggested that this species will decompose directly to HCN + $^\bullet$CH═CHCN and/or will open to $^\bullet$CH═N−CH═CH−CN and then decompose to HCN + $^\bullet$CH═CHCN[1]. These two channels were introduced to the reaction scheme.

C. Consecutive Free Radical Reactions. Except for the three initiation steps (reactions 1−3 in the kinetic scheme) that are unimolecular processes, all the reactions that compose the kinetics scheme involve free radicals. Figure 5 shows profiles of the free radicals in the system. The profiles were calculated for 1250 K, during a reaction time of 2 ms. As can be seen, $CH_3^\bullet$, $CH_2CN^\bullet$ $C_3H_3^\bullet$, CH═CHCN$^\bullet$, H$^\bullet$, and CN$^\bullet$ have the highest concentrations. They were introduced into the reaction scheme in abstraction and other reactions. $CH_3^\bullet$ is involved in abstractions and recombinations and is responsible for the production of species such as CH_4, C_2H_4, C_2H_6, CH_3CN, and others. H atoms play a very important role in the production of many of the species. $C_3H_3^\bullet$ is responsible for the production of allene and propyne. CN$^\bullet$ contributes, to some extent, to the formation of cyanogen.

2. Computer Modeling. ***A. Reaction Scheme.*** To model the observed product distribution, we have constructed the reaction scheme that is shown in Table 3. The scheme contains 33 species and 91 elementary reactions. The symbol **(R)** at the end of a reaction in the scheme indicates that the reverse reaction takes place. The rate constants listed in the table are given as $k = A \exp(-E/RT)$, or $k = A'T^n \exp(-E/RT)$ when the rate constant fits a wide temperature range. Units are cm^3, s^{-1}, kcal, and mol^{-1}. The Arrhenius parameters for the reactions in the scheme are either estimated or taken from various literature sources. These sources are specific articles relevant to the present issue, and databases, mainly the NIST-Kinetic Standard Reference Data Base 17.[6] The parameters for the reactions that were taken from the NIST-Kinetics Data Base are, in many cases, best fits to a large number of entries. The thermodynamic properties of the species involved were also taken from specific articles and various literature sources.[7−9] Some were estimated using NIST—Standard Reference Data Base 25[10] (Structure and Properties program (SP)).

Figures 6−12 show experimental and calculated yields of fourteen products found in the post-shock mixtures. The symbols in the figures are the experimental yields and the lines are the best fits to the calculated points using the scheme shown in Table 3. The calculations were done at 25 K intervals and are shown as (+) on the lines. Cis and trans crotonitrile and vinylacetonitrile were treated as one species as they interisomerize quite rapidly. Also, pyrazine which was found in very small quantities was not taken into consideration in the kinetic scheme. The agreement between the calculations and the experimental results are generally good. For several products the agreement at the low-temperature end of the range, where the yields of the individual products do not exceed a few hundredths of one percent is not very good. We suspect that this is caused by residual minute background in the G. C. or in the transfer tubes that could not be accounted for properly. When the yields are less than one hundredth of one percent, even a small background can cause a serious disagreement. Also, the model calculation overestimates the yield of CH≡C−CN. The reaction to which the yield of CH≡C−CN is most sensitive is the reaction: CH═CHCN$^\bullet$ → H$^\bullet$ + CH≡C−CN. We have used for the back reaction of this step the rate constant of the reaction H$^\bullet$ + CH≡CH → CH_2═CH$^\bullet$ (slightly reduced). A decrease in the rate constant of this reaction could lead to a good agreement between the experimental and the calculated yield of CH≡C−CN.

B. Sensitivity Analysis. Table 4 shows the sensitivity of the products to elimination of specific reactions from the kinetic scheme at 1150 and 1350 K. It gives the percent change in the yield of a particular product as a result of eliminating a given reaction from the scheme. The calculations correspond to dwell times of 2 ms. Reactions that show an effect of less than 10% both at 1150 K and at 1350 K are not included in the table.

As expected, not all the elementary steps affect the product distribution in the sense that their elimination from the scheme affects the yield of at least one of the products. The majority of the elementary reactions that compose the scheme do not affect or have only a small effect on the distribution. It should be mentioned, however, that the sensitivity analysis is done by removing a single reaction at a time. When a group of reactions is eliminated from the scheme there can be a strong effect on particular products although the elimination of one step alone, as is shown in Table 4, might not have an affect at all. These reactions are left in the kinetic scheme also for completeness and applicability beyond the temperature range of the present investigation where they might be more important.

Removal of elementary steps that are the sole producers of a given product or are part of a consecutive chain that is the only route for a product formation, reduces the concentration of that product almost to zero. As has been mentioned before the formation of all the products are associated with free radical reactions. The most important initiation reaction is reaction 2 (Table 3) which produces methyl radicals. These radicals

TABLE 3: Reaction Scheme for the Decomposition of 4-Methylpyrimidine

No	Reactions	*A*	*E*	k_f(1250K)	k_r(1250K)	ΔS_r(1250K)	ΔH_r(1250K)	ref
1	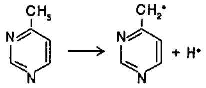	5.0×10^{15}	91.1	0.582	2.17×10^{13}	34.1	91.6	est (a)
2	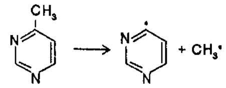	2.50×10^{16}	90.6	3.62	9.30×10^{12}	40.3	92.7	est (a)
3	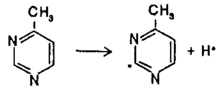	5.0×10^{15}	98.8	2.67×10^{-2}	4.49×10^{12}	39.1	101.6	est
4	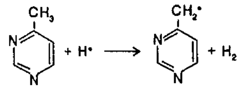	2.0×10^{14}	10	3.57×10^{12}	2.94×10^{8}	6.50	−15.2	est (a)
5	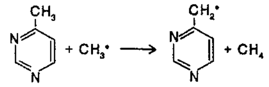	1.0×10^{13}	15	2.39×10^{10}	3.76×10^{7}	−0.081	−16.1	est (a)
6	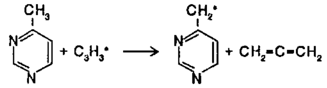	8.0×10^{11}	15	1.91×10^{9}	1.79×10^{9}	0.135	0.015	est
7	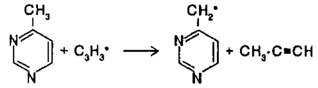	2.50×10^{12}	15	5.96×10^{9}	1.85×10^{9}	1.17	−1.45	est
8	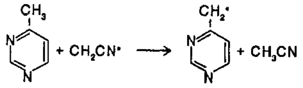	5.0×10^{12}	15	1.19×10^{10}	5.51×10^{9}	−0.361	−2.37	est
9	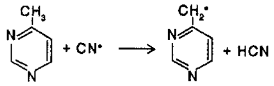	$2.0\times10^{5}T^{2.30}$	0	2.65×10^{12}	2.93×10^{5}	3.93	−34.9	est (b)
10	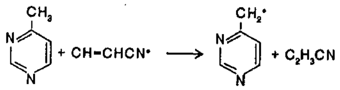	$1.36T^{3.65}$	5.17	3.42×10^{10}	1.26×10^{7}	2.96	−15.9	est (c)
11	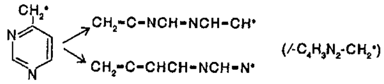	6.0×10^{14}	57	6.50×10^{4}	9.19×10^{9}	17.3	51	est
12	$l\text{-}C_4H_3N_2\text{–}CH_2^\bullet \rightarrow C_3H_3^\bullet + HCN + HCN$	3.0×10^{13}	32	7.63×10^{7}	9.01×10^{9}	58.1	27.1	est
13	$l\text{-}C_4H_3N_2\text{–}CH_2^\bullet \rightarrow CH_2CN^\bullet + C_2H_3CN$	5.0×10^{13}	32	1.27×10^{8}	4.53×10^{4}	25.6	−16.4	est
14	$l\text{-}C_4H_3N_2\text{–}CH_2^\bullet \rightarrow CH_2CN^\bullet + HCN + C_2H_2$	4.0×10^{13}	32	1.02×10^{8}	1.07×10^{10}	58.1	26.8	est
15	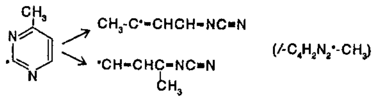	6.0×10^{14}	60	1.94×10^{4}	1.52×10^{10}	16.3	54	est
16	$l\text{-}C_4H_2N_2^\bullet\text{–}CH_3 \rightarrow p\text{-}C_3H_4 + HCN + CN^\bullet$	5.0×10^{13}	52	4.05×10^{4}	5.37×10^{11}	51.3	47.6	est
17	$l\text{-}C_4H_2N_2^\bullet\text{–}CH_3 \rightarrow C_2H_2 + CH_3CN + CN^\bullet$	5.0×10^{13}	52	4.05×10^{4}	7.15×10^{11}	49.8	46.4	est
18	$l\text{-}C_4H_2N_2^\bullet\text{–}CH_3 \rightarrow p\text{-}C_3H_4 + CHNCN^\bullet$	5.0×10^{13}	26	1.42×10^{9}	6.57×10^{11}	26.4	19.6	est
19	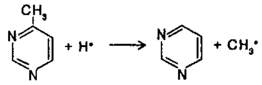	2.77×10^{13}	6.88	1.74×10^{12}	2.47×10^{9}	3.90	−11.4	est (a)
20	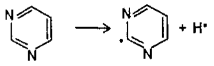	1.23×10^{15}	95	3.03×10^{-2}	7.31×10^{12}	36.4	99.1	1
21	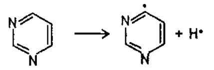	4.24×10^{15}	101	9.33×10^{-3}	1.68×10^{13}	36.4	104.1	1 (h)
22	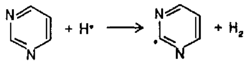	8.0×10^{13}	10	1.43×10^{12}	7.61×10^{8}	8.76	−7.77	est (d)

TABLE 3: (Continued)

No	Reactions	A	E	k_f(1250K)	k_r(1250K)	ΔS_r(1250K)	ΔH_r(1250K)	ref
23	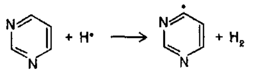	8.0×10^{13}	10	1.43×10^{12}	$5.70\text{x}10^{9}$	8.76	−2.77	est (d)
24	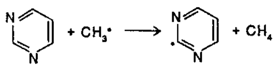	4.60×10^{12}	16	7.34×10^{9}	7.50×10^{7}	2.18	−8.66	est (e)
25	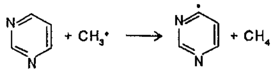	4.60×10^{12}	16	7.34×10^{9}	5.61×10^{8}	2.18	−3.66	est (e)
26	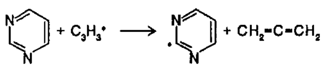	8.0×10^{11}	17	8.53×10^{8}	5.20×10^{9}	2.40	7.49	est
27	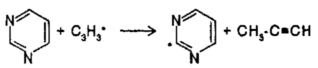	2.50×10^{12}	17	2.67×10^{9}	5.35×10^{9}	3.43	6.02	est
28	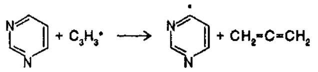	8.0×10^{11}	17	8.53×10^{8}	3.89×10^{10}	2.40	12.5	est
29	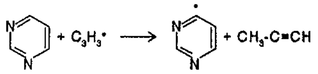	2.50×10^{12}	17	2.67×10^{9}	4.01×10^{10}	3.43	11	est
30	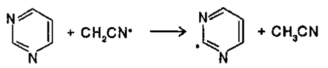	5.0×10^{12}	15	1.19×10^{10}	3.57×10^{10}	1.90	5.10	est
31	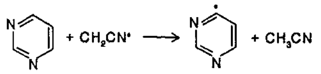	5.0×10^{12}	15	1.19×10^{10}	2.67×10^{11}	1.90	10.1	est
32	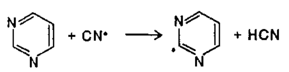	$2.0\times10^{5}T^{2.30}$	0	2.65×10^{12}	1.90×10^{6}	6.19	−27.4	1
33	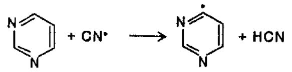	$3.98\times10^{5}T^{2.30}$	0	5.28×10^{12}	2.83×10^{7}	6.19	−22.4	1
34	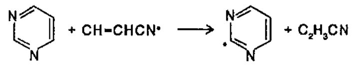	$1.36T^{3.65}$	5.17	3.42×10^{10}	8.15×10^{7}	5.22	−8.48	est
35	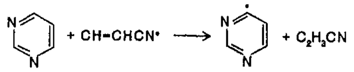	$1.36T^{3.65}$	5.17	3.42×10^{10}	6.10×10^{8}	5.22	−3.48	est
36	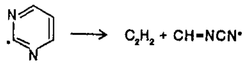	5.0×10^{13}	85	6.90×10^{-2}	2.36×10^{7}	47.1	79.1	est
37	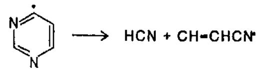	5.0×10^{13}	45	6.79×10^{5}	9.04×10^{8}	40.5	39.8	est
38	CH=NCN• + Ar → CN• + HCN + Ar	$3.63\times10^{27}T^{-3.66}$	25.6	5.62×10^{11}	1.61×10^{16}	24.9	28	1
39	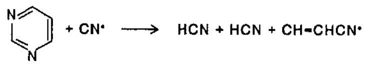	1.0×10^{13}	40	8.13×10^{6}	5.79×10^{4}	46.7	17.4	est
40	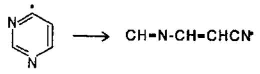	8.0×10^{15}	52	6.49×10^{6}	2.78×10^{8}	14.5	27.5	est
41	CH=N–CH=CHCN• → HCN + CH=CHCN•	1.0×10^{14}	15	2.39×10^{11}	7.41×10^{12}	26	12.4	4 (h)
42	CH=CHCN• → HC≡CCN + H•	1.0×10^{13}	52	8.11×10^{3}	1.47×10^{12}	23.9	48.5	est (f)
43	CH=CHCN• → C_2H_2 + CN•	5.0×10^{13}	62	724	7.15×10^{11}	31.5	62.2	est
44	CH=CHCN• + H• → C_2H_3CN	2.0×10^{14}	0	2.0×10^{14}	1.98×10^{-3}	−31.2	−107.6	est (g)

TABLE 3: (Continued)

No	Reactions	*A*	*E*	k_f(1250K)	k_r(1250K)	ΔS_r(1250K)	ΔH_r(1250K)	ref
45	$CH{=}CHCN^{\bullet} + H^{\bullet} \rightarrow C_2H_2 + HCN$	1.50×10^{14}	0	1.50×10^{14}	439	1.30	−64.3	est (g)
46	$CH{=}CHCN^{\bullet} + CN^{\bullet} \rightarrow C_2H_2 + C_2N_2$	1.0×10^{14}	0	1.0×10^{14}	274.	−5.18	−72.6	est (g)
47	$CH{=}CHCN^{\bullet} + CH{=}CHCN^{\bullet} \rightarrow HC{\equiv}CCN + C_2H_3CN$	2.50×10^{12}	6	2.23×10^{11}	399	−7.25	−59.1	est (g)
48	$CH{=}CHCN^{\bullet} + CH_3^{\bullet} \rightarrow C_3H_5CN^*$	5.0×10^{13}	0	5.0×10^{13}	2.68	−41.2	−98.7	est (g)
49	$CH{=}CHCN^{\bullet} + CH_3^{\bullet} \rightarrow CH_3CN + C_2H_2$	5.0×10^{13}	0	5.0×10^{13}	1.01×10^{5}	−5.84	−57	est (g)
50	$C_2N_2 + H^{\bullet} \rightarrow HCN + CN^{\bullet}$ **(R)**	3.16×10^{14}	8	1.26×10^{13}	1.35×10^{13}	6.49	8.27	11
51	$CN^{\bullet} + H_2 \rightarrow HCN + H^{\bullet}$	$3.60\times10^{8}T^{1.55}$	3	6.79×10^{12}	9.12×10^{9}	−2.57	−19.6	12
52	$C_2N_2 + Ar \rightarrow CN^{\bullet} + CN^{\bullet} + Ar$ **(R)**	4.11×10^{16}	93.5	1.85	6.67×10^{20}	36.7	134.8	13
53	$HCN + Ar \rightarrow H^{\bullet} + CN^{\bullet} + Ar$ **(R)**	4.57×10^{15}	105.2	1.85×10^{-3}	6.23×10^{17}	30.2	126.5	6
54	$C_2H_3CN \rightarrow C_2H_2 + HCN$	1.78×10^{12}	68	2.30	6.82×10^{5}	32.5	43.2	14
55	$C_2H_3CN \rightarrow HC{\equiv}CCN + H_2$	2.50×10^{13}	77	0.863	3.49×10^{7}	27.5	49.2	14
56	$C_2H_3CN + H^{\bullet} \rightarrow C_2H_3^{\bullet} + HCN$	5.0×10^{13}	8	2.0×10^{12}	2.66×10^{11}	8.67	5.84	4
57	$C_2H_3CN + H^{\bullet} \rightarrow H_2 + CH{=}CHCN^{\bullet}$ **(R)**	2.24×10^{14}	13.6	9.46×10^{11}	2.12×10^{11}	3.54	0.701	est
58	$CH_2CN^{\bullet} + CH_3^{\bullet} \rightarrow C_2H_5CN$	$5.0\times10^{14}T^{-0.50}$	0	1.41×10^{13}	169	−39.7	−83.4	15
59	$CH_3CN \rightarrow CH_2CN^{\bullet} + H^{\bullet}$ **(R)**	5.0×10^{15}	93	0.275	2.22×10^{13}	34.5	94	16
60	$CH_3CN + H^{\bullet} \rightarrow CH_3^{\bullet} + HCN$ **(R)**	2.0×10^{14}	2	8.94×10^{13}	1.30×10^{11}	7.14	−7.31	16
61	$CH_3CN + CH_3^{\bullet} \rightarrow CH_4 + CH_2CN^{\bullet}$	5.0×10^{12}	9	1.34×10^{11}	4.55×10^{8}	0.280	−13.8	16
62	$CH_3CN + H^{\bullet} \rightarrow H_2 + CH_2CN^{\bullet}$	1.38×10^{14}	9.54	2.97×10^{12}	5.28×10^{8}	6.86	−12.9	16
63	$CH_2CN^{\bullet} + C_2H_3^{\bullet} \rightarrow C_3H_5CN^*$ **(R)**	$6.0\times10^{13}T^{-0.50}$	0	1.70×10^{12}	1.24	−46	−98.3	15 (h)
64	$C_2H_5CN \rightarrow C_2H_4 + HCN$	6.0×10^{12}	72	1.55	4.89×10^{3}	32.6	32.1	15
65	$C_2H_5CN \rightarrow H_2 + C_2H_3CN$	2.51×10^{13}	77	0.867	8.01×10^{3}	31.6	33.6	15
66	$C_2H_5CN + H^{\bullet} \rightarrow C_2H_5^{\bullet} + HCN$	1.50×10^{14}	2	6.71×10^{13}	1.16×10^{11}	7.73	−6.14	15
67	$C_2H_5CN + H^{\bullet} \rightarrow C_2H_4CN^{\bullet} + H_2$	1.38×10^{14}	9.54	2.97×10^{12}	5.88×10^{9}	6.86	−6.89	15
68	$C_2H_5CN + CH_3^{\bullet} \rightarrow C_2H_4CN^{\bullet} + CH_4$	3.0×10^{13}	8	1.20×10^{12}	4.55×10^{10}	0.280	−7.78	15
69	$CH{=}NCN^{\bullet} + H^{\bullet} \rightarrow H_2 + C_2N_2$	3.97×10^{13}	0	3.97×10^{13}	2.36	−9.23	−87.2	1
70	$CH{=}NCN^{\bullet} + H^{\bullet} \rightarrow HCN + HCN$	3.15×10^{13}	0	3.15×10^{13}	2.68×10^{-3}	−5.31	−98.6	1
71	$CH{=}NCN^{\bullet} + CN^{\bullet} \rightarrow HCN + C_2N_2$	1.0×10^{14}	0	1.0×10^{14}	7.96×10^{-3}	−11.8	−106.8	1
72	$CH{=}NCN^{\bullet} + CH{=}CHCN^{\bullet} \rightarrow C_2N_2 + C_2H_3CN$	2.0×10^{13}	0	2.0×10^{13}	5.31	−12.8	−87.9	1
73	$C_2H_6 + H^{\bullet} \rightarrow C_2H_5^{\bullet} + H_2$	1.43×10^{14}	9.58	3.03×10^{12}	8.21×10^{9}	8.05	−4.62	6
74	$C_2H_5^{\bullet} \rightarrow C_2H_4 + H^{\bullet}$	6.21×10^{12}	38	1.43×10^{6}	2.60×10^{12}	24.9	38.3	6
75	$C_2H_3^{\bullet} + Ar \rightarrow C_2H_2 + H^{\bullet} + Ar$	3.0×10^{15}	32	7.54×10^{9}	1.67×10^{16}	23.8	37.4	17
76	$H^{\bullet} + H^{\bullet} + Ar \rightarrow H_2 + Ar$	$1.0\times10^{18}T^{-1.0}$	0	8.0×10^{14}	1.77×10^{-3}	−27.6	−106.9	18
77	$CH_3^{\bullet} + CH_3^{\bullet} \rightarrow C_2H_6$	$1.0\times10^{15}T^{-0.64}$	0	1.04×10^{13}	9.70	−40.3	−90.5	21
78	$CH_3^{\bullet} + CH_3^{\bullet} \rightarrow C_2H_5^{\bullet} + H^{\bullet}$	2.80×10^{13}	13.5	1.20×10^{11}	1.37×10^{14}	−4.56	11.8	19
79	$CH_3^{\bullet} + C_2H_4 \rightarrow CH_4 + C_2H_3^{\bullet}$	3.03×10^{13}	21.5	5.28×10^{9}	3.96×10^{10}	1.09	6.37	6
80	$CH_3^{\bullet} + C_2H_3^{\bullet} \rightarrow CH_4 + C_2H_2$	3.92×10^{11}	0	3.92×10^{11}	36.8	−10.4	−70.4	22
81	$CH_4 \rightarrow CH_3^{\bullet} + H^{\bullet}$ **(R)**	7.80×10^{14}	103.8	5.50×10^{-4}	1.30×10^{13}	34.2	107.8	6
82	$CH_4 + H^{\bullet} \rightarrow CH_3^{\bullet} + H_2$ **(R)**	$2.25\times10^{4}T^{3.0}$	8.76	1.29×10^{12}	6.75×10^{10}	6.58	0.886	22
83	$C_2H_4 + H^{\bullet} \rightarrow C_2H_3^{\bullet} + H_2$	2.63×10^{15}	20.7	6.37×10^{11}	2.49×10^{11}	7.67	7.25	6
84	$a\text{-}C_3H_4 \rightarrow p\text{-}C_3H_4$ **(R)**	1.48×10^{13}	60.4	408	134	1.03	−1.47	20
85	$a\text{-}C_3H_4 + Ar \rightarrow C_3H_3^{\bullet} + H^{\bullet} + Ar$ **(R)**	4.05×10^{17}	75.1	3.03×10^{4}	1.20×10^{18}	34	91.6	6
86	$p\text{-}C_3H_4 + Ar \rightarrow C_3H_3^{\bullet} + H^{\bullet} + Ar$ **(R)**	2.53×10^{17}	72.5	5.39×10^{4}	6.48×10^{18}	33	93.1	6
87	$C_2H_4CN^{\bullet} \rightarrow C_2H_3CN + H^{\bullet}$	3.0×10^{13}	40	3.05×10^{6}	1.42×10^{13}	24.8	40.5	16
88	$C_2H_4CN^{\bullet} + H^{\bullet} \rightarrow C_2H_5CN$ **(R)**	5.0×10^{12}	0	5.0×10^{12}	5.57×10^{-3}	−34.5	−100	15
89	$p\text{-}C_3H_4 + H^{\bullet} \rightarrow CH_3^{\bullet} + C_2H_2$ **(R)**	5.01×10^{13}	2	2.24×10^{13}	4.34×10^{10}	5.59	−8.53	15
90	$CH_3^{\bullet} + CN^{\bullet} \rightarrow CH_3CN$	5.0×10^{13}	0	5.0×10^{13}	1.02×10^{-4}	−37.4	−119.2	est
91	$C_2H_6 + CH_3^{\bullet} \rightarrow C_2H_5^{\bullet} + CH_4$	$0.548T^{4.0}$	8.28	4.77×10^{10}	2.48×10^{9}	1.47	−5.51	22

$C_3H_5CN^*$: cis, trans-$CH_3{-}CH{=}CHCN$ and $CH_2{=}CH{-}CH_2CN$

(a) based on the equivalent reactions of toluene (ref 6).

(b) based on the equivalent reaction of pyrimidine (ref 1).

(c) based on the reaction $C_2H_3 + C_4H_{10} \rightarrow C_2H_4 + C_4H_9^{\bullet}$ (ref 22).

(d) based on the equivalent reaction of C_6H_6 (ref 23).

(e) based on the equivalent reaction of C_6H_6 (ref 6).

(f) the back reaction is based on the reaction $H^{\bullet} + C_2H_2 \rightarrow C_2H_3^{\bullet}$ (ref 6).

(g) based on the equivalent reactions of $C_2H_3^{\bullet}$ (ref 6).

(h) slightly modified

TABLE 4: Sensitivity Spectrum: Percent Change in the Yield for Elimination a Step from the Reaction Scheme at 1170/1320 K

(a) Hydrocarbons

No	Reactions	CH_4	C_2H_2	C_2H_4	C_2H_6	$CH_2{=}C{=}CH_2$	$CH_3\text{–}C{\equiv}CH$
1	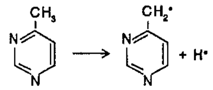	–	–	–10 / –29	–	–22 / –23	–20 / –23
2	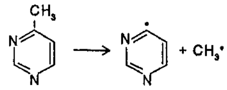	–93 / –90	–90 / –69	–99 / –97	–99 / –98	–76 / –58	–72 / –58
4	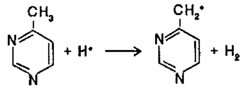	23 / 33	– / –20	61 / 59	53 / 98	–13 / –33	–10 / –32
5	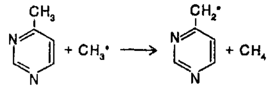	–99 / –68	–	222 / –	226 / 74	–39 / –23	–36 / –23
6	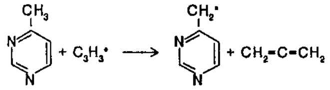	–	–	–	–	–93 / –31	–
7	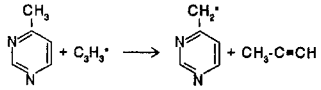	–	–	–	–	–	–87 / –43
8	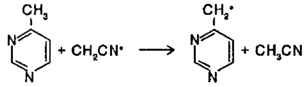	–	–	– / 26	–	– / –22	– / –22
10	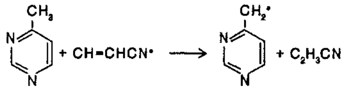	–	25 / –	–	–	–	–
11	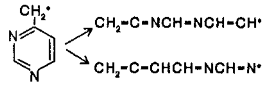 ($l\text{-}C_4H_3N_2\text{-}CH_2^{\bullet}$)	–	–41 / –63	– / –79	– / 97	–99 / –96	–92 / –94
12	$l\text{-}C_4H_3N_2\text{–}CH_2^{\bullet} \rightarrow C_3H_3^{\bullet} + HCN + HCN$	–	– / 20	– / 30	–	–99 / –95	–92 / –93
13	$l\text{-}C_4H_3N_2\text{–}CH_2^{\bullet} \rightarrow CH_2CN^{\bullet} + C_2H_3CN$	–	– / 38	– / –26	–	– / 53	– / 52
14	$l\text{-}C_4H_3N_2\text{–}CH_2^{\bullet} \rightarrow CH_2CN^{\bullet} + HCN + C_2H_2$	–	–42 / –64	–	–	– / 37	– / 36
19	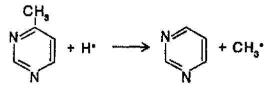	–	–	–22 / 16	–25 / –30	–	–
42	$CH{=}CHCN^{\bullet} \rightarrow HC{\equiv}CCN + H^{\bullet}$	–15 / –40	16 / 25	–31 / –75	–28 / –57	–	–
48	$CH{=}CHCN^{\bullet} + CH_3^{\bullet} \rightarrow C_3H_5CN^{*}$	–	–	17 / 23	16 / 20	–	–
49	$CH{=}CHCN^{\bullet} + CH_3^{\bullet} \rightarrow CH_3CN + C_2H_2$	–	–43 / –14	17 / 30	–	–	–
58	$CH_2CN^{\bullet} + CH_3^{\bullet} \rightarrow C_2H_5CN$	–	–	– / –83	– / 86	–	–
66	$C_2H_5CN + H^{\bullet} \rightarrow C_2H_5^{\bullet} + HCN$	–	–	– / –86	–	–	–
74	$C_2H_5^{\bullet} \rightarrow C_2H_4 + H^{\bullet}$	–	–	–99 / –95	–	–	–
77	$CH_3^{\bullet} + CH_3^{\bullet} \rightarrow C_2H_6$	– / 27	–	–	–100 / –99	–	–
78	$CH_3^{\bullet} + CH_3^{\bullet} \rightarrow C_2H_5^{\bullet} + H^{\bullet}$	–	–	–91 / –	–	–	–

(b) Nitrogen-Containing Species

No	Reactions	C_2N_2	HCN	$HC{\equiv}C\text{–}CN$	CH_3CN	C_2H_3CN	C_2H_5CN	$CH_3\text{–}CH{=}CHCN$	Pyrimidine
1	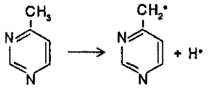	–	–	–	–	–	–24 / –19	–	–32 / –16
2	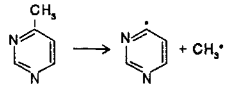	–99 / –96	–95 / –75	–99 / –99	–90 / –51	–95 / –63	–98 / –91	–99 / –99	–65 / –70

TABLE 4: (Continued)

(b) Nitrogen-Containing Species (Continued)

No	Reactions	C_2N_2	HCN	HC≡C–CN	CH_3CN	C_2H_3CN	C_2H_5CN	CH_3–CH=CHCN	Pyrimidine
4	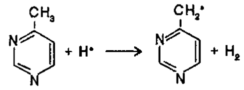	– / –21	–	–	– / –38	– / –33	– / –36	17 / 26	175 / 141
5	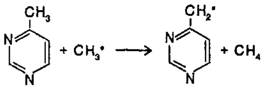	–20 / –16	–	–	–	–18 / –20	–	51 / 21	–
8	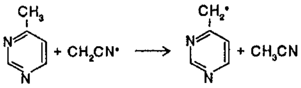	–	–	–	–39 / –69	– / –21	34 / 12	–	–
9	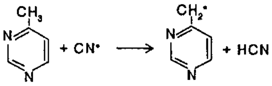	8959 / 260	–	–	–	–	–	–	–
10	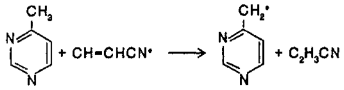	116 / –	–	60 / –	26 / –	–81 / –	–23 / –	57 / –	38 / –
11	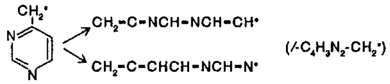	– / –42	–17 / –53	–	–39 / –65	–22 / –87	–99 / –98	– / 27	–
12	l-$C_4H_3N_2$–$CH_2^{\bullet} \rightarrow C_3H_3^{\bullet} + HCN + HCN$	–	–10 / –21	–	– / 20	– / 27	– / 25	–	–
13	l-$C_4H_3N_2$–$CH_2^{\bullet} \rightarrow CH_2CN^{\bullet} + C_2H_3CN$	–	– / 26	–	–21 / –18	–22 / –80	–53 / –25	–	–
14	l-$C_4H_3N_2$–$CH_2^{\bullet} \rightarrow CH_2CN^{\bullet} + HCN + C_2H_2$	–	–	–	–	– / 31	–42 / –17	–	–
19	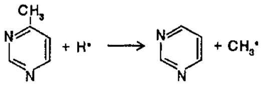	–	–	–	–	–	–	–	–99 / –99
38	$CH{=}NCN^{\bullet} + Ar \rightarrow CN^{\bullet} + HCN + Ar$	– / 23	–	–	–	–	–	–	–
42	$CH{=}CHCN^{\bullet} \rightarrow HC{\equiv}CCN + H^{\bullet}$	97 / 194	–	–99 / –99	15 / 30	37 / 11	–21 / –26	30 / 72	–65 / –69
43	$CH{=}CHCN^{\bullet} \rightarrow C_2H_2 + CN^{\bullet}$	–95 / –87	–	–	–	–	–	–	–
46	$CH{=}CHCN^{\bullet} + CN^{\bullet} \rightarrow C_2H_2 + C_2N_2$	–40 / –	–	–	–	–	–	–	–
48	$CH{=}CHCN^{\bullet} + CH_3^{\bullet} \rightarrow C_3H_5CN^*$	–	–	–	–	–	–	–100 / –99	–
49	$CH{=}CHCN^{\bullet} + CH_3^{\bullet} \rightarrow CH_3CN + C_2H_2$	–	–	–	–57 / –19	–	–	19 / 27	–
50	$C_2N_2 + H^{\bullet} \rightarrow HCN + CN^{\bullet}$ **(R)**	–40 / –82	–	–	–	–	–	–	–
58	$CH_2CN^{\bullet} + CH_3^{\bullet} \rightarrow C_2H_5CN$	–	–	–	– / 70	–	–99 / –99	– / 21	–

participate in the production of almost all the products, with and without nitrogen. Elimination of reaction 2 from the scheme reduces the yield of almost all the products almost to zero. This behavior is more emphasized at low temperatures. At the higher temperature end the effect slightly decreases owing to other channels that begin to contribute. Another interesting point is the effect of eliminating reaction 9 on the yield of cyanogen. Reaction 9 is the main consumption reaction of cyanogen radicals. When this reaction is eliminated from the scheme the concentration of cyanogen increases by orders of magnitude as recombination of the latter produces cyanogen.

We have also run sensitivity analysis with respect to variations (or rather uncertainties) in the $\Delta_f H^0$ of species whose thermodynamic properties were estimated or are not known accurately enough. An incorrect values of the thermodynamic functions result in erroneous values for the rate constants of the back reactions for a given value of the forward rate constant. In several sensitivity tests that were performed on uncertain values of heat of formation of various species, we found that the results of the computer simulations were only slightly sensitive to variations of ~3 kcal/mol in the values of the estimated $\Delta_f H^0$.

Acknowledgment. This work was supported by a grant from GIF (German Israel Foundation) for Scientific Research and Development.

References and Notes

(1) Kiefer, J. H.; Zhang, Q.; Kern, R. D.; Yan, J.; Jursic, B. *J. Phys. Chem. A* **1997**, *101*, 7061−7073.

(2) Kiefer, J. H.; Zhang, Q.; Kern, R. D.; Chen, H.; Yao, J.; Jursic, B. *Proc. Combust. Inst.* **1996**, *26*, 651.

(3) Doughty, A.; Mackie, J. C.; Palmer, J. M. *Proc. Combust. Inst.* **1994**, *25*, 893.

(4) Doughty, A.; Mackie, J. C. *J. Chem. Soc., Faraday Trans.* **1994**, *90* (4), 541−548.

(5) Tsang, W.; Lifshitz, A. *Int. J. Chem. Kinet.* **1998**, *30*, 621.

(6) Westly, F.; Herron, J. T.; Cvetanovic, R. J.; Hampson, R. F.; Mallard, W. G. *NIST−Chemical Kinetics Standard Reference Database 17*, Version 5.0; National Institute of Standards and Technology: Washington, DC.

(7) Pedley, J. B.; Taylor, R. D.; Kirby, S. P. *Thermochemical Data of Organic Compounds*; Chapman and Hall: London, 1986.

(8) Burcat, A.; McBride, B.; Rabinowitz, M. Ideal Gas Thermodynamic Data for Compounds Used in Combustion. T. A. E. 657 Report; Technion−Israel Institute of Technology: Haifa, Israel, 1997.

(9) Warnatz, J. In Rate coefficients in the C/H/O system. *Combustion Chemistry*; Gardiner, W. C., Jr., Ed.; Springer-Verlag: New York, 1984.

(10) Stein, S. E.; Rukkers, J. M.; Brown, R. L. *NIST−Standard Reference Database 25*; National Institute of Standards and Technology: Washington, DC.

(11) Louge, M. Y.; Hanson, R. K. *Combust. Flame* **1984**, *58*, 291.

(12) Tsang, W. *J. Phys. Chem. Ref. Data*, **1992**, *21*, 753−791.

(13) Colket, M. B., III *Int. J. Chem. Kinet*. **1984**, *16*, 353.

(14) Lifshitz, A.; Bidani, M.; Suslensky, A.; Tamburu, C. *J. Phys. Chem*. **1989**, *93*, 1369.

(15) Lifshitz, A.; Shweky, I.; Tamburu, C. *J. Phys. Chem.* **1993**, *97*, 4442−4449.

(16) Lifshitz, A.; Tamburu, C. *J. Chem. Kinet.* **1998**, *30*, 341−347.

(17) Warnatz, J. Rate coefficients in the C/H/O system. In Combustion Chemistry"; Gardiner, W. C., Jr., Ed.; Springer-Verlag: New York, 1984.

(18) Jacobs, T. A.; Giedt, R. R.; Cohen, N. *J. Chem. Phys*. **1967**, *47*, 54−57.

(19) Frank, P.; Braun-Unkhoff, M. Proceedings of the 16th International Symposium on Shock Tubes and Waves, Aachen, 1987; VCH: Weinheim, Germany, 1988; p 83.

(20) Lifshitz, A.; Frenklach, M.; Burcat, A. *J. Phys. Chem*. **1975**, *79*, 1148.

(21) Tsang, W. *Combust. Flame* **1989**, *78*, 71−86.

(22) Tsang, W.; Hampson, R. F. *J. Phys. Chem. Ref. Data*, **1986**, *15*, 1087.

(23) Nicovich, J. M.; Ravishankara, A. R. *J. Phys. Chem.*, **1984**, *88*, 2534.